Macromolecules

pubs.acs.org/Macromolecules Article

Breaking the Paradox between Grafting-Through and Depolymerization to Access Recyclable Graft Polymers

Zeyu Wang,† Seiyoung Yoon,† and Junpeng Wang*

Cite This: *Macromolecules* 2022, 55, 9249−9256 Read Online

ACCESS | Metrics & More | Article Recommendations | Supporting Information

ABSTRACT: Graft polymers, owing to their grafted structures, possess unique properties useful for a broad range of applications. Due to the demand for a circular economy, it is desirable to have graft polymers depolymerizable. However, depolymerizable graft polymers are rare, and existing examples of depolymerizable graft polymers lack the rigor in controlling the size and architecture. Herein, we demonstrate a robust method to synthesize depolymerizable graft polymers by leveraging our recent development of chemically recyclable polymers prepared from controlled ring-opening metathesis polymerization of *trans*-cyclobutane fused *trans*-cyclooctenes. The superior reactivity of the highly strained *trans*-cyclooctene allows grafting-through of macromonomers to be successfully conducted, empowering excellent control in backbone length for various types of sidechains, including a poly(ethylene glycol), a polylactide, and an aliphatic chain. Notably, an ultrahigh molecular weight of 14 000 kDa is achieved with high conversion (>90%) and low dispersity ($Đ$ < 1.2). The controlled polymerization enables the synthesis of graft polymers of various architectures, including block and statistical copolymers. Kinetic studies of depolymerization show that the graft polymers depolymerize to the *cis*-cyclooctene macromonomers through an unzipping mechanism. The versatile synthesis of depolymerizable graft polymers opens the door to sustainable thermoplastics with diverse material properties.

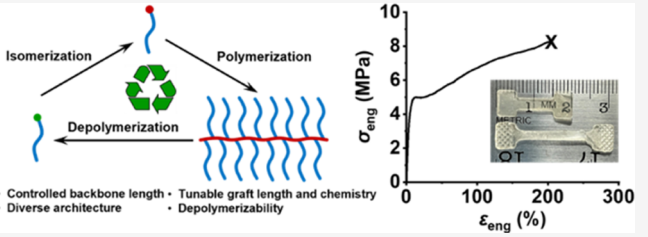

INTRODUCTION

Graft polymers are a class of macromolecules with grafted sidechains,[1] affording unique properties that are useful for numerous technologies, such as touch sensors,[2,3] tissue-mimicking elastomers,[4−7] and photonic crystals.[8−10] The graft architecture can be achieved through three methods: grafting-to, grafting-from, and grafting-through (Figure 1a). Both grafting-to and grafting-from methods are based on a preformed polymer backbone, and the sidechain is formed either by attaching a polymer to the polymer backbone using a coupling reaction (grafting-to) or by growing polymer chains from initiators on the polymer backbone (grafting-from).[11−16] While grafting-to is advantageous in that it allows for separate preparation and characterization of the backbone and the sidechain,[17−20] due to steric hindrance, grafting becomes progressively more difficult as conversion increases, leading to limited grafting density. Compared to the grafting-to route, grafting-from typically renders improved control in grafting density, but the efficiency of the initiators on the polymer backbone could be affected by the high density of initiation sites.[19,21,22] In addition, it is not straightforward to prepare more complex architectures, such as graft block copolymers, from either grafting-to or grafting-from methods.[23] The grafting-through approach starts with a macromonomer (MM) that comprises a monomer and a polymer chain: polymerization of the monomer forms the backbone, and the polymer chain on the MM becomes the sidechain of the corresponding graft copolymer. Compared to the other two methods, grafting-through is advantageous in its facile and precise control over the backbone length, sidechain types and length, grafting density, and polymer architecture, provided that the polymerization of the MM is well controlled.

It is important to note that the long sidechain in a MM would inevitably reduce the effective concentration of the propagating moiety, which requires the polymerization chemistry to be highly exergonic. Examples of polymerization chemistry for grafting-through include polyaddition of olefins[24] and ring-opening metathesis polymerization (ROMP) of norbornene derivatives.[25] Because of the mild reaction conditions, excellent functional group tolerance, and ease of operation, along with the abovementioned benefits of grafting-through, ROMP of norbornene-derived MMs has become the most widely used method for accessing graft polymers.[8,25−30] Nevertheless, the exergonic nature of the polymerization used for grafting-through also makes the corresponding graft polymers non-depolymerizable (Figure 1b), limiting the

Received: August 2, 2022
Revised: September 27, 2022
Published: October 14, 2022

https://doi.org/10.1021/acs.macromol.2c01609
Macromolecules 2022, 55, 9249−9256

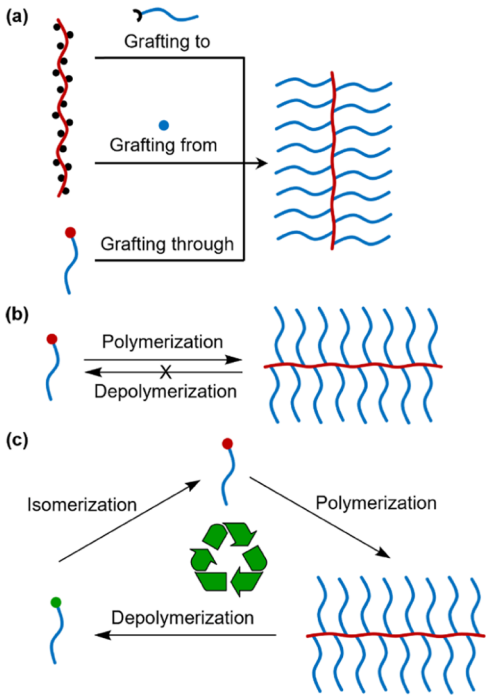

Figure 1. (a) Three grafting approaches to graft polymers. (b) Highly exergonic grafting-through method disfavors depolymerization. (c) Isomerization of *t*CB*c*CO-MM into *t*CB*t*CO-MM increases the driving force of polymerization, and the resulting graft polymer can be depolymerized back to *t*CB*c*CO-MM.

sustainable use of these materials. Existing depolymerizable graft polymers typically lack robustness in controlling their architecture, functionality, and size.[31−35] For example, the depolymerizable polycyclopentene bottlebrushes based on the grafting-from approach require delicate temperature control during the synthesis of the backbone; in addition, monomer conversion needed to be limited at a low level (<10%) during the synthesis of the sidechain to obtain narrow molecular weight distribution.[34,36] Depolymerizable graft polymers have also been prepared using controlled radical polymerizations of MMs, but these reactions have limited efficiencies and accessible molecular weights.[32,33,35]

We recently reported a series of ROMP polymers based on *trans*-cyclobutane fused cyclooctene (*t*CBCO) monomers, in which the additional ring reduces the ring strain energy of the cyclooctene monomer to such a level that the polymerization becomes reversible.[37] The *t*CBCO polymers can undergo efficient depolymerization in the presence of a metathesis catalyst under mild conditions. Compared to other depolymerization systems, this system is unique in that the *cis*-cyclooctene monomer, i.e., *t*CB*c*CO, can be isomerized into its *trans* analogue, *t*CB*t*CO, allowing for the driving force of polymerization to be temporarily elevated so that controlled polymerization can be achieved at monomer concentrations as low as 25 mM.[38] We envisioned that the highly exergonic polymerization of *t*CB*t*CO and the depolymerizability of the resulting polymer could make this system suitable for accessing depolymerizable graft polymers via the grafting-through approach (Figure 1c). Herein, we report the synthesis of graft polymers by grafting-through of MMs with a *t*CB*t*CO end group. The living ROMP of the *t*CB*t*CO is found to be robust enough to overcome the low concentration and steric effects caused by the long sidechains in MMs, affording controlled polymerization. Controlled synthesis of graft polymers is demonstrated for three different types of sidechains, including a poly(ethylene glycol), a polylactide, and an aliphatic chain. Various polymer architectures of graft copolymers are achieved, including a block copolymer and a statistical

Scheme 1. Synthesis of *t*CB*t*CO-Bearing Macromonomers

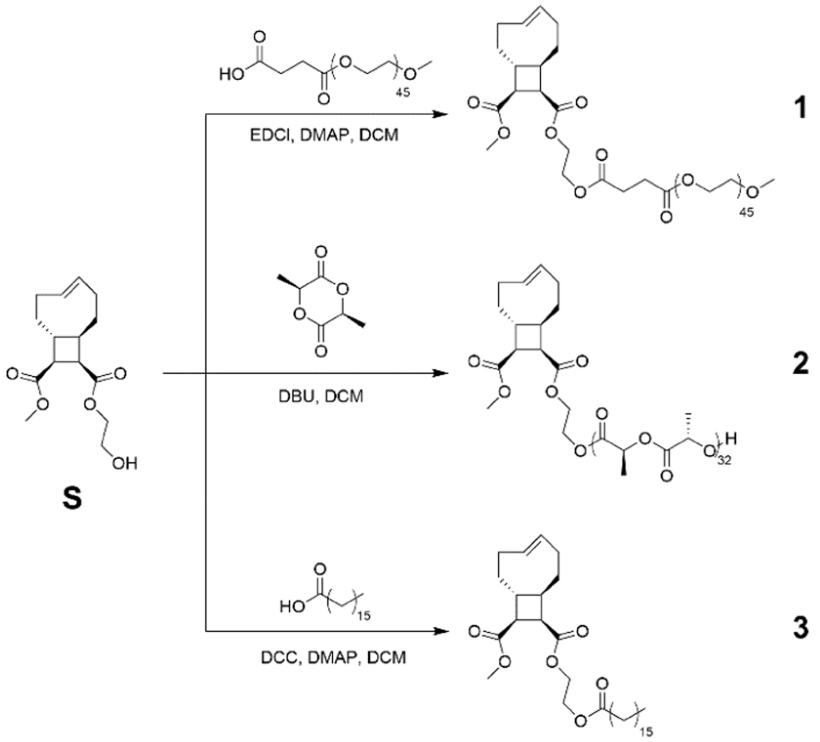

https://doi.org/10.1021/acs.macromol.2c01609
Macromolecules 2022, 55, 9249−9256

Table 1. Synthesis and Characterization of Graft Copolymers

entry	MM_x	MM_y	type	$[MM_x]_0/[\mathbf{G1}]_0$:$[MM_y]_0/[\mathbf{G1}]_0$[a]	conversion[b] (%)	$M_{n,theo}$ (kDa)[c]	M_n (kDa)[d]	$Đ$[d]
1	**1**		homo	100	97	229	312	1.05
2	**2**		homo	100	95	465	526	1.01
3	**2**		homo	500	98	2396	2161	1.08
4	**2**		homo	1000	97	4743	5341	1.02
5	**2**		homo	2000	96	9389	10 280	1.09
6	**2**		homo	3000	95	13 937	14 350	1.17
7	**3**		homo	100	98	54	68	1.12
8	**3**	**1**	block	100:10	98	76	221	1.15
9	**2**	**3**	statistical	300:2700	96	2795	3654	1.10

[a]Molar ratio of MM to **G1**. [b]Calculated from SEC-RI by comparing the peak areas of graft polymer and residual MM (including unreacted *t*CB*t*CO-MM and any *t*CB*c*CO-MM) for entries 1−6, and from ^{1}H NMR spectroscopy by comparing the olefin integrations of graft polymer and residual MM (including unreacted *t*CB*t*CO-MM and any *t*CB*c*CO-MM) for entries 7−9. [c]Theoretical M_n based on MM-to-**G1** ratio and corrected with conversion. [d]Determined by SEC-RI/MALS in dimethylformamide (DMF) with 0.01 M LiBr for entry 1 and in THF for the others.

copolymer, and from the latter was prepared a ductile thermoplastic material. Kinetic studies of depolymerization show that the graft polymers depolymerize through an unzipping pathway.

RESULTS AND DISCUSSION

Synthesis of *t*CB*t*CO Macromonomers. An MM includes two components that are covalently connected: a monomer moiety and a polymer chain; it can be synthesized either by directly coupling the polymer chain end with the monomer moiety or by growing the polymer chain from an initiator that is attached to the monomer. Since a hydroxy group can link with a CO_2H-terminated polymer through esterification or serve as an initiator for ring-opening polymerization, we synthesized a hydroxyl-functionalized *t*CB*t*CO **S** (Scheme 1; for details, see the Supporting Information) as the precursor for MMs. Three MMs with distinct sidechains—including poly(ethylene glycol) (PEG, 2 kDa) (**1**), poly(L-lactide) (PLLA) (**2**), and a long fatty acid (**3**)—were prepared (Scheme 1). MMs **1** and **3** were synthesized via Steglich esterification of **S** with mPEG-CO_2H and margaric acid, respectively. MM **2** was obtained by polymerization of L-lactide using **S** as the initiator and 1,8-diazabicyclo[5.4.0]undec-7-ene (DBU) as the organocatalyst.[39] The ring-opening transesterification polymerization of L-lactide proceeded in a controlled fashion (Figures S13 and S14). The number-average molecular weight (M_n) of **2** obtained from end-group analysis using ^{1}H NMR agreed well with that obtained from size-exclusion chromatography (SEC) coupled with a refractive index (RI) detector and a multi-angle light scattering (MALS) detector (Table S1, entry 2). Matrix-assisted laser desorption ionization time-of-flight mass spectrometry confirmed the high chain-end fidelity of both **1** and **2** (Figures S9 and S15).

Controlled Grafting-Through ROMP of *t*CB*t*CO Macromonomers. We commenced the experiments from the ROMP of **1** (Table 1, entry 1) using previously optimized conditions for other *t*CB*t*CO monomers.[38] The polymerization was conducted at a concentration of $[\text{olefin}]_0$ = 0.025 M in degassed THF at room temperature. Grubbs 1st generation catalyst (**G1**) was used as the initiator, and triphenylphosphine (PPh_3) was added to suppress secondary metathesis and depolymerization. The initial **1**/**G1**/PPh_3 molar ratio was set at 100/1/30. After proceeding for 90 min, the ROMP was quenched by ethyl vinyl ether (EVE). The polymerization was found to reach a full consumption of *t*CB*t*CO based on ^{1}H NMR (Figure S19). A residual MM peak (3%) was observed in the SEC-RI trace, which could be attributed to the tiny fraction of *t*CB*c*CO already present in **1**, which can be readily removed from the crude product through dialysis against H_2O (Figure S20). The resulting graft copolymer possessed a narrow molecular weight distribution ($Đ$ = 1.05) and a number-average molecular weight M_n of 312 kDa.

Having established success in polymerizing a *t*CB*t*CO MM, we were interested in investigating the kinetics of polymerization. Polymerizations of both **1** and **2** were conducted under conditions similar to the initial trial described above, except that the polymerization of **2** was carried out in a THF/$CHCl_3$ (1/4 v/v) mixture due to limited solubility of PLLA in pure THF. Aliquots were taken from the ROMP mixtures during the polymerizations and were added to excess EVE in separate vials for termination. The polymerizations for both **1** and **2** reached high conversions (>90%) within 15 min (Figure 2a). Pseudo-first-order kinetics, reflected from the linear relationship between $\ln[M]_0/[M]_t$ and time, was observed for the polymerization of **2** (Figure 2a), indicating fast initiation and efficient suppression of depolymerization by PPh_3. For ROMP of both **1** and **2**, M_n increased proportionally to conversions (Figure 2b), confirming little or no secondary metathesis as a result of excess PPh_3. Narrow and monomodal molecular weight distributions ($Đ$ < 1.2) were also observed throughout the course of ROMP (Figures 2b, S21 and S24). Consistent with the observations for the linear architecture,[38] while a coordinating solvent such as THF is essential to ensure controlled polymerization, the inclusion of another solvent did not affect the control of the polymerization. While the coordinating solvent THF is supposed to not only suppress the secondary metathesis but also slow down the propagation during the ROMP of *t*COs,[40] the ROMP of **1** conducted in THF proceeded faster than the ROMP of **2** in a mixture of THF and $CHCl_3$, possibly due to the lower molecular weight of **1**.

Another characteristic of controlled polymerization is the ability to tune the molecular weight by varying the monomer-to-initiator ratio. Five polymerizations were conducted with $[\mathbf{2}]_0/[\mathbf{G1}]_0$ ratios ranging from 100 to 3000. The polymerizations were allowed to proceed for 2 h before being quenched with EVE. As the **2**-to-**G1** ratio increased, the resulting **P2** peak shifted toward a shorter retention time in SEC (Figure 3a), and the absolute molecular weight obtained from SEC-RI/MALS increased proportionally, matching well with the dashed line indicating theoretical molecular weights

https://doi.org/10.1021/acs.macromol.2c01609
Macromolecules 2022, 55, 9249−9256

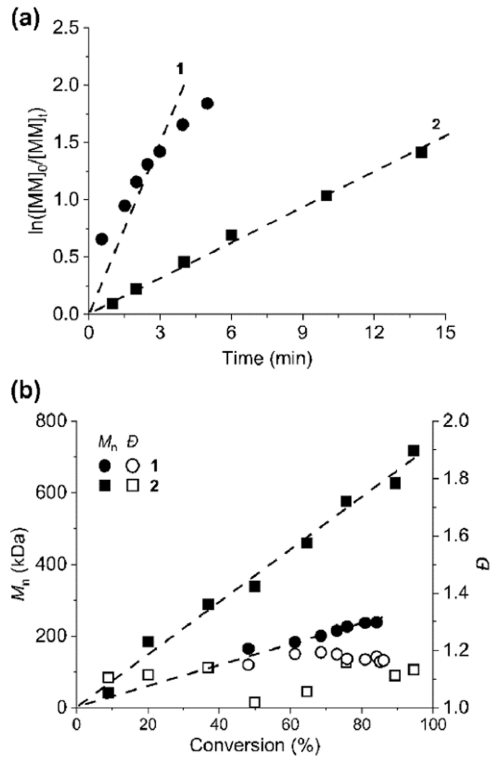

Figure 2. Grafting-through ROMP kinetics of **1** (circles) and **2** (squares) at $[MM]_0/[\mathbf{G1}]_0/[PPh_3]_0$ = 100/1/30 and $[MM]_0$ = 0.025 M at room temperature: (a) $\ln([MM]_0/[MM]_t)$ as a function of time; (b) M_n (solid) and $Đ$ (hollow) over conversion.

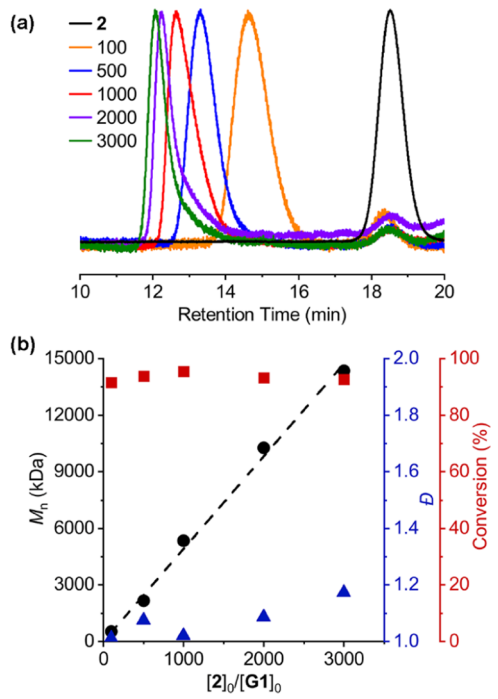

Figure 3. Backbone length control in the ROMP of **2** at $[\mathbf{G1}]_0/[PPh_3]_0$ = 1/30 and $[MM]_0$ = 0.025 M in THF/$CHCl_3$ (1/4) at room temperature: (a) SEC-RI (THF) traces of polymerization mixture with varying $[\mathbf{2}]_0/[\mathbf{G1}]_0$ ratios; (b) M_n, conversion and $Đ$ at different $[\mathbf{2}]_0/[\mathbf{G1}]_0$ ratios, with the dashed line representing theoretical M_n increase over $[\mathbf{2}]_0/[\mathbf{G1}]_0$ ratios.

(Figure 3b). Significantly, this linear increase held valid up to an ultrahigh degree of polymerization (DP) of 3000, corresponding to an M_n of 14 000 kDa.[26] The high ring strain and low hindrance of the *t*CB*t*CO moiety rendered nearly quantitative consumption of **2** and low dispersities in all $[\mathbf{2}]_0/[\mathbf{G1}]_0$ ratios tested. This is in contrast to norbornene-based MMs, which suffer from reduced conversion with increasing MM-to-initiator ratio to varying extents, depending on the anchoring group chemistry.[41] The capability of accessing ultrahigh molecular weight graft polymers in a controlled fashion makes the *t*CB*t*CO grafting-through system appealing for applications where well-defined, large-size graft polymers are desirable.

Synthesis and Self-Assembly of *t*CB*t*CO Graft Block Copolymer. Encouraged by the controlled polymerization that produced well-defined graft homopolymers, we further set out to synthesize a block copolymer via sequential addition of two different MMs. We were interested in obtaining a block copolymer that can undergo microphase separation to form nanostructures, such as lamellae. Hence, we chose **1** and **3** as our monomers for their presumably high Flory–Huggins interaction parameter χ. ROMP of **3** was conducted with an initial $\mathbf{3}/\mathbf{G1}/PPh_3$ ratio of 100/1/30 and allowed to proceed for 10 min, at which point a THF solution of **1** (10 equiv. to **G1**) was added. The polymerization of **1** was allowed to proceed for an additional 20 min before being quenched with EVE. NMR analyses confirmed the sequential consumption of both MMs at high conversions (98% for both **3** and **1**) (Figure S28). The resulting polymer **P3-*b*-P1** was purified via prep-GPC, followed by dialysis against MeOH. According to ^{1}H NMR analysis, the incorporation ratio of **3** and **1** was 9.1:1, which is close to the feed ratio of 10:1. Although the SEC peak of **P3-*b*-P1** appeared at a longer retention time than that of the first block **P3** (Figure S29), SEC-RI/MALS characterization showed an increase in the absolute molecular weight from **P3** to **P3-*b*-P1** (Table S2, entry 8). While it is not clear to us why the absolute molecular weight of the **P3-*b*-P1** was much higher than the theoretical value, the abnormal retention time observed for **P3-*b*-P1** was likely due to the PEG-column lone pair-π interactions. The block architecture (Figure 4a) was further supported by differential scanning calorimetry (DSC) studies, which showed two melting temperatures (T_m) for **P3-*b*-P1** at 19.0 and 48.6 °C (Figure S44), matching well with the melting temperatures of the corresponding homopolymers—T_ms for **P3** and **P1** are 17.9 and 48.4 °C respectively (Figures S42 and S37). The presence of two distinguishable melting temperatures supports the block architecture.

To assess the bulk assembly of the graft block copolymer, a sample of **P3-*b*-P1** was annealed in bulk at 75 °C for 5 h, followed by quenching at 25 °C for 48 h. Small-angle X-ray scattering (SAXS) of the self-assembled sample revealed a domain spacing ($d = 2\pi/q^*$) of 40.7 nm, which is commensurate with that of a graft block copolymer with comparable molecular weight and volume ratio.[42] This relatively large spacing further confirmed the block structure, as a random copolymer would otherwise result in sidechain segregation and a much smaller domain spacing.[27] In addition, the SAXS pattern showed four orders of scattering peaks with relative angular positions of 1:2:3:4 (Figure 4b). The SAXS pattern here suggests well-ordered lamellar morphology, which is normally observed for more balanced volume ratios.[42,43] Given the very asymmetric volume fraction for the two blocks—71 and 29% for **P3** and **P1**, respectively, the lamellar

https://doi.org/10.1021/acs.macromol.2c01609
Macromolecules 2022, 55, 9249–9256

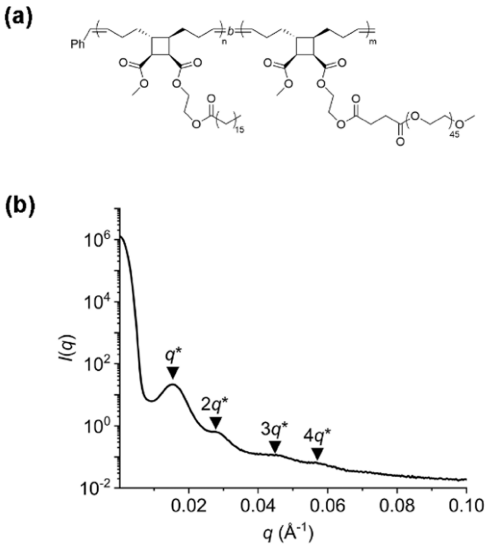

Figure 4. (a) Chemical structure of **P3**-*b*-**P1** and (b) its SAXS profile (at room temperature) indicating a lamellar morphology with a domain spacing $d = 2\pi/q^* = 40.7$ nm.

morphology could be due to the unique graft architecture, which provides rich opportunities for accessing a variety of microphase separation patterns. In the future, we will leverage the capability of controlling the size and volume fraction of this system to systematically investigate the self-assembly of the graft copolymers.

Depolymerization of Graft Polymer. Depolymerization of *t*CB*t*CO graft polymers was tested with **P1**. A solution of **P1** with $[\text{olefin}]_0$ = 0.01 M and 1 mol % **G2** in toluene was degassed and then heated at 50 °C while stirring in a nitrogen atmosphere overnight. ^{1}H NMR showed that the macromonomer was not *t*CB*t*CO MM **1** but the *cis*-cyclooctene form (Figure 5a), which is reasonable due to the high ring strain energy of the *trans*-cyclooctene. The selective formation of the low-strain *cis*-cyclooctene isomer during depolymerization is consistent with our previous observation with the linear *t*CB*t*CO polymers.[38] SEC-RI traces revealed that **P1** was completely consumed after depolymerization and macromonomer along with a small fraction of oligomers formed (Figure 5b).

To further understand the depolymerization process, we studied the depolymerization kinetics of **P1** using SEC. As the depolymerization proceeded, the fraction of **P1** decreased, and the SEC peak of **P1** disappeared after 15 min of depolymerization. The fraction of oligomers increased in the beginning and reached a maximum of ∼40% before gradually decreasing (Figure 6b), similar to the trend shown during the depolymerization of *t*CBCO linear polymers.[37] Most of the oligomers were converted into the monomer after 130 min of depolymerization, at which point, the fractions of oligomers and macromonomers were 7 and 93%, respectively. Notably, the molecular weight of the residual **P1** (retention time 20−24.5 min) did not decrease significantly until the very late stage of depolymerization (Figure 6a,c), when the solution contains primarily the *t*CB*c*CO macromonomer and oligomers. For example, the reduction in M_n is less than 30%, even at 80% of depolymerization. Similar to the observation by Kennemur and co-workers on their depolymerization study of the graft polypentenamers,[34] the slow molecular weight reduction of the residual **P1** rules out a random chain scission

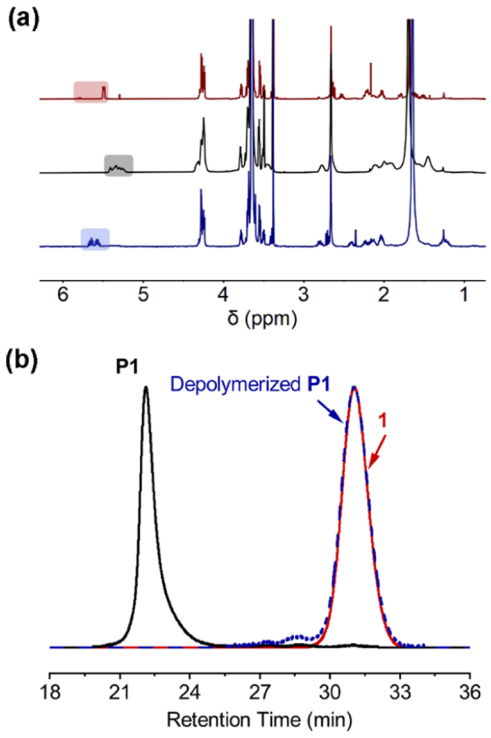

Figure 5. Depolymerization of **P1** at [olefin] = 0.01 M in toluene at 50 °C with 1 mol % **G2** overnight: (a) ^{1}H NMR spectra ($CDCl_3$) of **1** (top), **P1** (middle), and depolymerization products of **P1** (bottom); (b) SEC-RI (DMF with 0.01 M LiBr) traces of **1** (red solid line), **P1** (black solid line), and depolymerized **P1** (blue dashed line).

mechanism—which would lead to exponential decay in molecular weight (Figure 6c, blue dashed line)—and suggests an end-to-end unzipping mechanism.[37] On the other hand, if all of the chains underwent unzipping depolymerization simultaneously, the M_n would show a linear decrease with the percentage of depolymerization (Figure 6c, red dashed line). The observed slow molecular weight reduction, therefore, suggests that at each time, only a very low fraction of chains underwent depolymerization, most likely limited by the slow coordination of the Ru catalyst to the chain end due to the steric hindrance in the densely grafted architecture.[34]

Recyclable Thermoplastics Based on Graft Copolymer. The depolymerizability of our system provides an opportunity to develop sustainable thermoplastics based on the graft architecture, which, compared to linear polymers, can access more diverse properties.[44−47] We expected that a statistical copolymer of **P2** and **P3** (Figure 7a) would form a thermoplastic material since the glassy/semicrystalline **P2** would act as the physical cross-linking point and the molten **P3** would bridge the hard domains (Figures S41 and S42). A $[\mathbf{2}]_0/[\mathbf{3}]_0/[\mathbf{G1}]_0$ ratio of 300/2700/1 was used for ROMP, and the polymerization was quenched by EVE at 3 h, affording a conversion of 96%. The resulting polymer showed a narrow molecular weight distribution, and its M_n is close to the theoretical value (Table 1, entry 9). The resulting polymer **P2**-*stat*-**P3** was purified by precipitation in cold diethyl ether. NMR analysis revealed that the molar ratio of incorporated **2** and **3** is 1:9.9, close to the feed ratio, 9:1, corresponding to a mass ratio of 13:12. The copolymer was able to undergo facile depolymerization into a compostable short PLLA and a *t*CB*c*CO-based fatty acid molecule (Figures S34 and S35), the

https://doi.org/10.1021/acs.macromol.2c01609
Macromolecules 2022, 55, 9249−9256

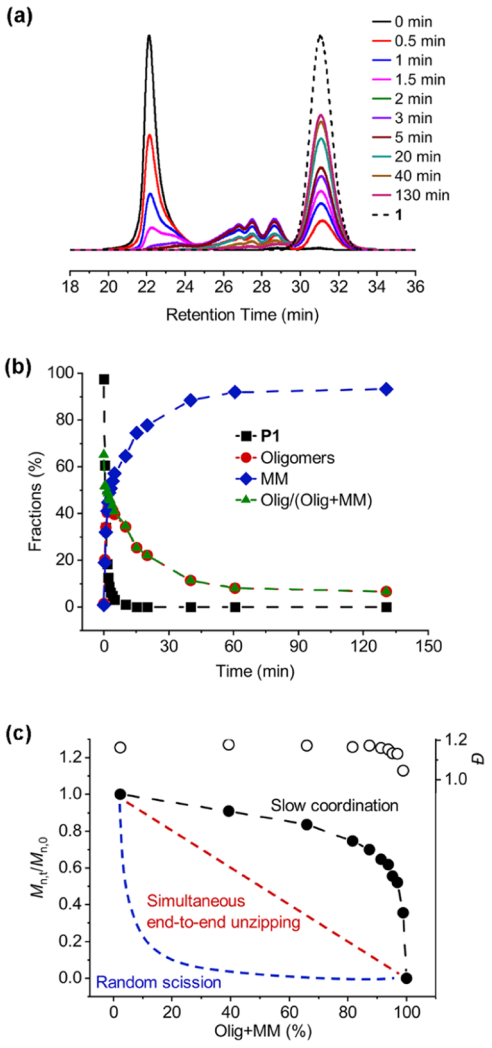

Figure 6. Depolymerization kinetic study of **P1** at [olefin] = 0.01 M in toluene at 50 °C in the presence of 1 mol % **G2**: (a) SEC-RI (DMF with 0.01 M LiBr) traces of aliquots drawn from the reaction mixture at different times; (b) fractions of remaining **P1** (black squares), oligomers (red circles), MM (blue diamonds), and oligomers/(oligomers + MM) (green triangles) as a function of depolymerization time; (c) normalized M_n of **P1** ($M_{n,t}$:M_n of the remaining **P1** during depolymerization, $M_{n,0}$:M_n of the initial **P1**) (filled circles) and $Đ$ of the remaining **P1** (hollow circles) as a function of depolymerization percentage.

latter of which can be photochemically isomerized to its *trans* analogue (Figure S17).

X-ray scattering was employed to gain further insight into the morphological features (Figure S47). The presence of a broad principal SAXS peak suggests microphase separation, while the absence of higher-order peaks excludes well-ordered structure (e.g., lamellar morphology). The domain spacing (17 nm) is similar to what was observed for brush random copolymers with comparable graft length,[27] supporting a random instead of tapered/gradient copolymer composition, which would result in a much larger domain spacing.[48] Elevating the temperature to 180 °C significantly weakened and broadened the SAXS peak due to disordering. By cooling the sample to 38 °C, a narrower peak was found at the same q value, suggesting that a stronger microphase separation was recovered.[44]

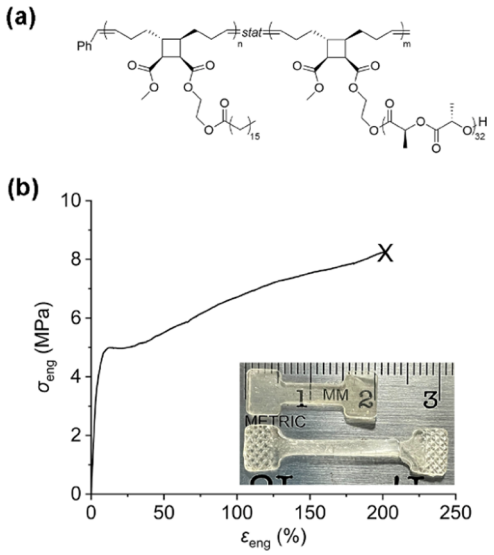

Figure 7. (a) Chemical structure of **P2-*stat*-P3** and (b) a representative stress−strain curve of a dumbbell specimen of **P2-*stat*-P3** under uniaxial extension. Inset: representative examples of unstretched (left) and stretched (right) dumbbell specimens.

Mechanical properties of the thermoplastic graft copolymer were evaluated by uniaxial extension testing on dogbone specimens prepared through compression molding at 170 °C. Average values of the tensile properties were obtained from four replicates: Young's modulus (130 ± 18 MPa), yield stress (4.4 ± 0.4 MPa), and stress at break (8.5 ± 0.3 MPa). These values are comparable to those of low-density polyethylene: Young's modulus (280 ± 40 MPa), yield stress (8 ± 1 MPa), and stress at break (10 ± 2 MPa MPa),[49] suggesting the potential of using *t*CB*t*CO-based graft copolymers as sustainable thermoplastics. Shown in Figure 7b is a representative stress−strain curve (more curves are shown in Figure S48) of a dumbbell specimen extended at a cross-head speed of 5 mm/min. The specimen underwent an initially linear elastic deformation, followed by yielding and further elongation until failure at three times its original length. The ruptured specimen remained about twice its original length, suggesting comparable portions of elastic and plastic deformation.

CONCLUSIONS

The conflicting thermodynamic demand between grafting-through and depolymerization is addressed using *t*CB*t*CO-based macromonomers, in which the *trans*-cyclooctene enables highly endergonic living polymerization for grafting-through while the *trans*-cyclobutane fused ring makes depolymerization favorable by reducing the ring strain energy of the cyclooctene. The grafting-through of the *t*CB*t*CO-based macromonomers represents a rare case where depolymerizable graft polymers can be accessed while the size, functionality, and architecture of the graft polymers can be precisely controlled. These capabilities, along with the demonstrated mechanical testing, make the *t*CB*t*CO graft copolymers promising candidates for developing recyclable plastic materials with diverse properties.

https://doi.org/10.1021/acs.macromol.2c01609
Macromolecules 2022, 55, 9249−9256

■ ASSOCIATED CONTENT

Supporting Information

The Supporting Information is available free of charge at https://pubs.acs.org/doi/10.1021/acs.macromol.2c01609.

Synthetic procedures, polymerization studies, depolymerization studies, NMR spectra, mass spectrometry, TGA and DSC curves, SEC traces, SAXS curves, and tensile testing data (PDF)

■ AUTHOR INFORMATION

Corresponding Author

Junpeng Wang − *School of Polymer Science and Polymer Engineering, the University of Akron, Akron, Ohio 44325, United States;* orcid.org/0000-0002-4503-5026; Email: jwang6@uakron.edu

Authors

Zeyu Wang − *School of Polymer Science and Polymer Engineering, the University of Akron, Akron, Ohio 44325, United States;* orcid.org/0000-0002-6343-0548

Seiyoung Yoon − *School of Polymer Science and Polymer Engineering, the University of Akron, Akron, Ohio 44325, United States;* orcid.org/0000-0002-2961-1505

Complete contact information is available at: https://pubs.acs.org/10.1021/acs.macromol.2c01609

Author Contributions

†Z.W. and S.Y. contributed equally to this work. The manuscript was written through contributions of all authors. All authors have given approval to the final version of the manuscript.

Notes

The authors declare no competing financial interest.

■ ACKNOWLEDGMENTS

This material is based upon work supported by the University of Akron and the National Science Foundation under Grant No. DMR-2042494. The authors thank Kayla Williams-Pavlantos and Prof. Chrys Wesdemiotis for mass spectrometry analysis, Prof. James Eagan for glovebox access, and Prof. Mark Foster for advice on X-ray scattering measurements. The authors acknowledge access to the X-ray scattering facility at the Advanced Materials and Liquid Crystal Institute (AMLCI) at Kent State University, which was financially supported by the National Science Foundation (DMR-2017845), the State of Ohio (The Ohio Department of Higher Education Action Fund), and Kent State University. The authors thank The Ohio Board of Regents and The National Science Foundation (CHE-0341701 and DMR-0414599) for the funds used to purchase the NMR instrument used in this work.

■ REFERENCES

(1) Sheiko, S. S.; Sumerlin, B. S.; Matyjaszewski, K. Cylindrical Molecular Brushes: Synthesis, Characterization, and Properties. *Prog. Polym. Sci.* **2008**, *33*, 759−785.

(2) Reynolds, V. G.; Mukherjee, S.; Xie, R.; Levi, A. E.; Atassi, A.; Uchiyama, T.; Wang, H.; Chabinyc, M. L.; Bates, C. M. Super-Soft Solvent-Free Bottlebrush Elastomers for Touch Sensing. *Mater. Horiz.* **2020**, *7*, 181−187.

(3) Xiong, H.; Zhang, L.; Wu, Q.; Zhang, H.; Peng, Y.; Zhao, L.; Huang, G.; Wu, J. A Strain-Adaptive, Self-Healing, Breathable and Perceptive Bottle-Brush Material Inspired by Skin. *J. Mater. Chem. A* **2020**, *8*, 24645−24654.

(4) Vatankhah-Varnosfaderani, M.; Daniel, W. F. M.; Everhart, M. H.; Pandya, A. A.; Liang, H.; Matyjaszewski, K.; Dobrynin, A. V.; Sheiko, S. S. Mimicking Biological Stress-Strain Behaviour with Synthetic Elastomers. *Nature* **2017**, *549*, 497−501.

(5) Keith, A. N.; Vatankhah-Varnosfaderani, M.; Clair, C.; Fahimipour, F.; Dashtimoghadam, E.; Lallam, A.; Sztucki, M.; Ivanov, D. A.; Liang, H.; Dobrynin, A. V.; Sheiko, S. S. Bottlebrush Bridge between Soft Gels and Firm Tissues. *ACS Cent. Sci.* **2020**, *6*, 413−419.

(6) Zhang, D.; Dashtimoghadam, E.; Fahimipour, F.; Hu, X.; Li, Q.; Bersenev, E. A.; Ivanov, D. A.; Vatankhah-Varnoosfaderani, M.; Sheiko, S. S. Tissue-Adaptive Materials with Independently Regulated Modulus and Transition Temperature. *Adv. Mater.* **2020**, *32*, No. 2005314.

(7) Dashtimoghadam, E.; Fahimipour, F.; Keith, A. N.; Vashahi, F.; Popryadukhin, P.; Vatankhah-Varnosfaderani, M.; Sheiko, S. S. Injectable Non-Leaching Tissue-Mimetic Bottlebrush Elastomers as an Advanced Platform for Reconstructive Surgery. *Nat. Commun.* **2021**, *12*, No. 3961.

(8) Sveinbjörnsson, B. R.; Weitekamp, R. A.; Miyake, G. M.; Xia, Y.; Atwater, H. A.; Grubbs, R. H. Rapid Self-Assembly of Brush Block Copolymers to Photonic Crystals. *Proc. Natl. Acad. Sci. U.S.A.* **2012**, *109*, 14332−14336.

(9) Guo, T.; Yu, X.; Zhao, Y.; Yuan, X.; Li, J.; Ren, L. Structure Memory Photonic Crystals Prepared by Hierarchical Self-Assembly of Semicrystalline Bottlebrush Block Copolymers. *Macromolecules* **2020**, *53*, 3602−3610.

(10) Zhao, T. H.; Jacucci, G.; Chen, X.; Song, D. P.; Vignolini, S.; Parker, R. M. Angular-Independent Photonic Pigments via the Controlled Micellization of Amphiphilic Bottlebrush Block Copolymers. *Adv. Mater.* **2020**, *32*, No. 2002681.

(11) Beers, K. L.; Gaynor, S. G.; Matyjaszewski, K.; Sheiko, S. S.; Möller, M. The Synthesis of Densely Grafted Copolymers by Atom Transfer Radical Polymerization. *Macromolecules* **1998**, *31*, 9413−9415.

(12) Börner, H. G.; Beers, K.; Matyjaszewski, K.; Sheiko, S. S.; Möller, M. Synthesis of Molecular Brushes with Block Copolymer Side Chains Using Atom Transfer Radical Polymerization. *Macromolecules* **2001**, *34*, 4375−4383.

(13) Cheng, G.; Böker, A.; Zhang, M.; Krausch, G.; Müller, A. H. E. Amphiphilic Cylindrical Core-Shell Brushes via a "Grafting from" Process Using ATRP. *Macromolecules* **2001**, *34*, 6883−6888.

(14) Zhang, M.; Breiner, T.; Mori, H.; Müller, A. H. E. Amphiphilic Cylindrical Brushes with Poly(Acrylic Acid) Core and Poly(n-Butyl Acrylate) Shell and Narrow Length Distribution. *Polymer* **2003**, *44*, 1449−1458.

(15) Kriegel, R. M.; Rees, W. S.; Weck, M. Synthesis and Hydrolysis of Poly(Norbornene)/Poly(Acrylic Acid) Graft Copolymers Synthesized via a Combination of Atom-Transfer Radical Polymerization and Ring-Opening Metathesis Polymerization. *Macromolecules* **2004**, *37*, 6644−6649.

(16) Runge, M. B.; Dutta, S.; Bowden, N. B. Synthesis of Comb Block Copolymers by ROMP, ATRP, and ROP and Their Assembly in the Solid State. *Macromolecules* **2006**, *39*, 498−508.

(17) Deffieux, A.; Schappacher, M. Synthesis and Characterization of Star and Comb Polystyrenes Using Isometric Poly(Chloroethyl Vinyl Ether) Oligomers as Reactive Backbone. *Macromolecules* **1999**, *32*, 1797−1802.

(18) Schappacher, M.; Deffieux, A. From Combs to Comb-g-Comb Centipedes. *Macromolecules* **2005**, *38*, 7209−7213.

(19) Gao, H.; Matyjaszewski, K. Synthesis of Molecular Brushes by "Grafting onto" Method: Combination of ATRP and Click Reactions. *J. Am. Chem. Soc.* **2007**, *129*, 6633−6639.

(20) Schappacher, M.; Deffieux, A. Synthesis of Macrocyclic Copolymer Brushes and Their Self-Assembly into Supramolecular Tubes. *Science* **2008**, *319*, 1512−1516.

(21) Neugebauer, D.; Sumerlin, B. S.; Matyjaszewski, K.; Goodhart, B.; Sheiko, S. S. How Dense Are Cylindrical Brushes Grafted from a Multifunctional Macroinitiator? *Polymer* **2004**, *45*, 8173−8179.
(22) Sumerlin, B. S.; Neugebauer, D.; Matyjaszewski, K. Initiation Efficiency in the Synthesis of Molecular Brushes by Grafting from via Atom Transfer Radical Polymerization. *Macromolecules* **2005**, *38*, 702−708.
(23) Bolton, J.; Rzayev, J. Synthesis and Melt Self-Assembly of PS−PMMA−PLA Triblock Bottlebrush Copolymers. *Macromolecules* **2014**, *47*, 2864−2874.
(24) Neugebauer, D.; Zhang, Y.; Pakula, T.; Sheiko, S. S.; Matyjaszewski, K. Densely-Grafted and Double-Grafted PEO Brushes via ATRP. A Route to Soft Elastomers. *Macromolecules* **2003**, *36*, 6746−6755.
(25) Xia, Y.; Kornfield, J. A.; Grubbs, R. H. Efficient Synthesis of Narrowly Dispersed Brush Polymers via Living Ring-Opening Metathesis Polymerization of Macromonomers. *Macromolecules* **2009**, *42*, 3761−3766.
(26) Jha, S.; Dutta, S.; Bowden, N. B. Synthesis of Ultralarge Molecular Weight Bottlebrush Polymers Using Grubbs' Catalysts. *Macromolecules* **2004**, *37*, 4365−4374. Ultrahigh molecular weight graft polymers synthesized from grafting-through have been reported but the polymerization was less controlled; their graft polymers with higher molecular weights were obtained by grafting-from method
(27) Xia, Y.; Olsen, B. D.; Kornfield, J. A.; Grubbs, R. H. Efficient Synthesis of Narrowly Dispersed Brush Copolymers and Study of Their Assemblies: The Importance of Side Chain Arrangement. *J. Am. Chem. Soc.* **2009**, *131*, 18525−18532.
(28) Kawamoto, K.; Zhong, M.; Gadelrab, K. R.; Cheng, L. C.; Ross, C. A.; Alexander-Katz, A.; Johnson, J. A. Graft-through Synthesis and Assembly of Janus Bottlebrush Polymers from A-Branch-B Diblock Macromonomers. *J. Am. Chem. Soc.* **2016**, *138*, 11501−11504.
(29) Guo, Z. H.; Le, A. N.; Feng, X.; Choo, Y.; Liu, B.; Wang, D.; Wan, Z.; Gu, Y.; Zhao, J.; Li, V.; Osuji, C. O.; Johnson, J. A.; Zhong, M. SI - Janus Graft Block Copolymers: Design of a Polymer Architecture for Independently Tuned Nanostructures and Polymer Properties. *Angew. Chem., Int. Ed.* **2018**, *57*, 8493−8497.
(30) Guo, Z. H.; Le, A. N.; Feng, X.; Choo, Y.; Liu, B.; Wang, D.; Wan, Z.; Gu, Y.; Zhao, J.; Li, V.; Osuji, C. O.; Johnson, J. A.; Zhong, M. Janus Graft Block Copolymers: Design of a Polymer Architecture for Independently Tuned Nanostructures and Polymer Properties. *Angew. Chem., Int. Ed.* **2018**, *57*, 8493−8497.
(31) Xiao, Y.; Li, H.; Zhang, B.; Cheng, Z.; Li, Y.; Tan, X.; Zhang, K. Modulating the Depolymerization of Self-Immolative Brush Polymers with Poly(Benzyl Ether) Backbones. *Macromolecules* **2018**, *51*, 2899−2905.
(32) Flanders, M. J.; Gramlich, W. M. Reversible-Addition Fragmentation Chain Transfer (RAFT) Mediated Depolymerization of Brush Polymers. *Polym. Chem.* **2018**, *9*, 2328−2335.
(33) Martinez, M. R.; Dadashi-Silab, S.; Lorandi, F.; Zhao, Y.; Matyjaszewski, K. Depolymerization of P(PDMS11MA) Bottlebrushes via Atom Transfer Radical Polymerization with Activator Regeneration. *Macromolecules* **2021**, *54*, 5526−5538.
(34) Neary, W. J.; Isais, T. A.; Kennemur, J. G. Depolymerization of Bottlebrush Polypentenamers and Their Macromolecular Metamorphosis. *J. Am. Chem. Soc.* **2019**, *141*, 14220−14229.
(35) Wang, H. S.; Truong, N. P.; Pei, Z.; Coote, M. L.; Anastasaki, A. Reversing RAFT Polymerization: Near-Quantitative Monomer Generation Via a Catalyst-Free Depolymerization Approach. *J. Am. Chem. Soc.* **2022**, *144*, 4678−4684.
(36) Neary, W. J.; Fultz, B. A.; Kennemur, J. G. Well-Defined and Precision-Grafted Bottlebrush Polypentenamers from Variable Temperature ROMP and ATRP. *ACS Macro Lett.* **2018**, *7*, 1080−1086.
(37) Sathe, D.; Zhou, J.; Chen, H.; Su, H.-W.; Xie, W.; Hsu, T.-G.; Schrage, B. R.; Smith, T.; Ziegler, C. J.; Wang, J. Olefin Metathesis-Based Chemically Recyclable Polymers Enabled by Fused-Ring Monomers. *Nat. Chem.* **2021**, *13*, 743−750.
(38) Chen, H.; Shi, Z.; Hsu, T.-G.; Wang, J. Overcoming the Low Driving Force in Forming Depolymerizable Polymers through Monomer Isomerization. *Angew. Chem., Int. Ed.* **2021**, *60*, 25493−25498.
(39) Lohmeijer, B. G. G.; Pratt, R. C.; Leibfarth, F.; Logan, J. W.; Long, D. A.; Dove, A. P.; Nederberg, F.; Choi, J.; Wade, C.; Waymouth, R. M.; Hedrick, J. L. Guanidine and Amidine Organocatalysts for Ring-Opening Polymerization of Cyclic Esters. *Macromolecules* **2006**, *39*, 8574−8583.
(40) Walker, R.; Conrad, R. M.; Grubbs, R. H. The Living ROMP of Trans-Cyclooctene. *Macromolecules* **2009**, *42*, 599−605.
(41) Radzinski, S. C.; Foster, J. C.; Chapleski, R. C.; Troya, D.; Matson, J. B. Bottlebrush Polymer Synthesis by Ring-Opening Metathesis Polymerization: The Significance of the Anchor Group. *J. Am. Chem. Soc.* **2016**, *138*, 6998−7004.
(42) Gai, Y.; Song, D. P.; Yavitt, B. M.; Watkins, J. J. Polystyrene-Block-Poly(Ethylene Oxide) Bottlebrush Block Copolymer Morphology Transitions: Influence of Side Chain Length and Volume Fraction. *Macromolecules* **2017**, *50*, 1503−1511. The graft block copolymer that was referred to, Sk-28, has a molecular weight of 320.2 kg/mol and f_{PEO} of 28%
(43) Bates, F. S.; Fredrickson, G. H. Block Copolymers-Designer Soft Materials. *Phys. Today* **1999**, *52*, 32−38.
(44) Fournier, L.; Mirabal, R.; Hillmyer, D. M.; Toward, M. A. Sustainable Elastomers from the Grafting-Through Polymerization of Lactone-Containing Polyester Macromonomers. *Macromolecules* **2022**, *55*, 1003−1014.
(45) Zhang, J.; Li, T.; Mannion, A. M.; Schneiderman, D. K.; Hillmyer, M. A.; Bates, F. S. Tough and Sustainable Graft Block Copolymer Thermoplastics. *ACS Macro Lett.* **2016**, *5*, 407−412.
(46) Zhang, J.; Schneiderman, D. K.; Li, T.; Hillmyer, M. A.; Bates, F. S. Design of Graft Block Polymer Thermoplastics. *Macromolecules* **2016**, *49*, 9108−9118.
(47) Zhou, C.; Wei, Z.; Jin, C.; Wang, Y.; Yu, Y.; Leng, X.; Li, Y. Fully Biobased Thermoplastic Elastomers: Synthesis of Highly Branched Linear Comb Poly(β-Myrcene)-Graft-Poly(L-Lactide) Copolymers with Tunable Mechanical Properties. *Polymer* **2018**, *138*, 57−64.
(48) Jiang, L.; Nykypanchuk, D.; Ribbe, A. E.; Rzayev, J. One-Shot Synthesis and Melt Self-Assembly of Bottlebrush Copolymers with a Gradient Compositional Profile. *ACS Macro Lett.* **2018**, *7*, 619−623.
(49) Teator, A. J.; Leibfarth, F. A. Catalyst-Controlled Stereoselective Cationic Polymerization of Vinyl Ethers. *Science* **2019**, *363*, 1439−1443.

https://doi.org/10.1021/acs.macromol.2c01609
Macromolecules 2022, 55, 9249−9256